https://doi.org/10.5194/egusphere-2026-4237
Preprint. Discussion started: 2 September 2026
© Author(s) 2026. CC BY 4.0 License.

Ice-sheet evolution controlled by meltwater connectivity across ice-shelf gaps

Franka Jesse[1], Erwin Lambert[2], Constantijn J. Berends[1], and Roderik S.W. van de Wal[1,2,3]

[1]Institute for Marine and Atmospheric Research Utrecht, Utrecht University, Princetonplein 5, 3584 CC Utrecht, The Netherlands
[2]Royal Netherlands Meteorological Institute (KNMI), Utrechtseweg 297, 3731 GA, De Bilt, The Netherlands
[3]Department of Physical Geography, Utrecht University, Utrecht, 3584 CB, The Netherlands

Correspondence: Franka Jesse (t.f.jesse@uu.nl)

Abstract. In regions of intense sub-shelf melting, ice shelves can substantially weaken, potentially leading to the formation of gaps within the ice shelf. Using a coupled ice-sheet–meltwater-layer model, we investigate two end-member representations of meltwater transport across such gaps: meltwater either exits the cavity (sink) or remains dynamically connected across ice-free regions (connected). For an idealised ice-sheet–ice-shelf geometry based on the MISMIP+ framework, our results show that gaps form under both moderate (0°C at depth) and warm (1°C at depth) ocean forcing, driven by enhanced melting associated with a strong western boundary current. When gaps are treated as sinks, downstream melting is suppressed. In contrast, retaining meltwater connectivity allows heat and momentum to propagate downstream, enhancing further ice-shelf thinning along the western shear margin. This thinning reduces stress transmission between the ice shelf and the grounded ice, resulting in greater ice-volume loss in the connected configuration. The difference in ice-volume loss between the two meltwater representations can be comparable in magnitude to that caused by a 1°C increase in ocean temperature forcing. These results highlight meltwater connectivity across ice-shelf gaps as an important source of uncertainty in projections of ice-sheet evolution and mass loss.

1 Introduction

Understanding ocean-driven ice-shelf melting, hereafter referred to as sub-shelf melting, is essential for improving projections of future Antarctic ice mass loss (Pritchard et al., 2012). The ocean circulation within ice-shelf cavities is primarily buoyancy driven (Lewis and Perkin, 1986). Warm, saline water enters the cavity at depth and reaches the ice-shelf base near the grounding line, where it drives the formation of a buoyant, relatively fresh meltwater layer. This meltwater then rises along the ice-shelf base towards the open ocean under the influence of buoyancy. Melt rates depend on both thermal driving and friction velocity within the meltwater layer (Holland and Jenkins, 1999). As a result, melt patterns are highly heterogeneous, with enhanced melting typically occurring near grounding lines, where thermal driving is strongest, and within basal channels or along Coriolis-favoured shear margins (Zinck et al., 2026), where flow is intensified by topographic steering and Coriolis deflection, respectively.

https://doi.org/10.5194/egusphere-2026-4237
Preprint. Discussion started: 2 September 2026
© Author(s) 2026. CC BY 4.0 License.

Under sufficiently strong ocean forcing, enhanced sub-shelf melting can locally thin ice shelves to the point of increased fracture likelihood (Watkins et al., 2024) or complete melt-through (Wearing et al., 2021), thereby creating gaps within the ice shelf. How the sub-shelf meltwater circulation responds to the formation of such gaps is poorly understood. If these regions remain open to the atmosphere, they may act as effective sinks for the meltwater layer, allowing heat and momentum to be dissipated as the plume exits the cavity. Alternatively, the formation of fast ice, potentially promoted by the exposure to cold atmospheric conditions and the presence of fresh meltwater at the surface (Fraser et al., 2023), could limit the exchange between the meltwater layer and the atmosphere. In that case, the meltwater circulation may remain dynamically connected across these gaps, allowing meltwater to traverse downstream to the other side of the gap with relatively little disruption.

Because sub-shelf melt rates depend on the persistence of heat and momentum within the meltwater layer, the treatment of the meltwater layer in such gaps may have important implications for downstream melting and, ultimately, the ice-dynamical response of the system. The assumption that gaps in the ice shelf act as a direct sink for the meltwater layer is incorporated in the default configuration of the one-Layer Antarctic model for Dynamical Downscaling of Ice–ocean Exchanges (LADDIE) (Lambert et al., 2023). Previous work coupling LADDIE to an ice-sheet model demonstrated that this sink can reduce sub-shelf melting downstream of the gap and consequently lead to a slowdown in ice retreat over time (Jesse et al., 2025).

In this study, we use a coupled configuration of the meltwater-layer model LADDIE version 2.0 (Lambert et al., 2026) and the ice-sheet model UFEMISM version 2.0 (Berends et al., 2025) to quantify the sensitivity of sub-shelf melt patterns and the ice-dynamical response to different representations of meltwater flow across ice-shelf gaps. We compare two end-member cases: a sink scenario, in which heat and momentum are removed in open areas (the default in LADDIE and the configuration used by Jesse et al. (2025)), and a connected scenario, in which the meltwater layer remains dynamically continuous across ice-shelf gaps. Across a range of idealised ocean states and model resolutions, we assess how the two representations impact sub-shelf melt patterns and ice-sheet evolution.

2 Methods

2.1 Model description

2.1.1 Meltwater layer model LADDIE

We use the meltwater layer model LADDIE version 2.0 (Lambert et al., 2026), which resolves buoyancy-driven circulation within the well-mixed meltwater layer based on two-dimensional, depth-averaged plume dynamics (Holland and Feltham, 2006). The model is discretised on an unstructured mesh and solves the depth-integrated Navier–Stokes equations to compute the horizontal velocities, thickness, temperature, and salinity of the meltwater layer. Sub-shelf melt rates are calculated using the three-equation formulation (Holland and Jenkins, 1999; Jenkins et al., 2010), in which melting depends on the friction velocity and thermal driving within the meltwater layer. At the base of the layer, entrainment is included as a volumetric source term. By integrating all variables forward in time, the model evolves toward a quasi-steady state of the meltwater flow and corresponding sub-shelf melt rates for a prescribed ice-shelf geometry and ambient ocean forcing.

https://doi.org/10.5194/egusphere-2026-4237
Preprint. Discussion started: 2 September 2026
© Author(s) 2026. CC BY 4.0 License.

By default, LADDIE treats open areas that form within the initial ice-shelf domain as a calving front (Fig. 1a). At the calving front, the open boundary conditions between ice-covered and ice-free cells allow heat and momentum to escape the cavity. Consequently, when a meltwater current encounters such a gap, its heat and momentum are removed from the system, preventing them from propagating downstream. This approach, however, represents an extreme scenario. It assumes these areas lose heat as rapidly as the open ocean, whereas gaps within an ice shelf are often more sheltered and may be covered by sea ice (Lilien et al., 2018). The resulting insulation would limit heat and momentum loss to the atmosphere, suggesting that the sub-shelf meltwater layer may actually remain continuous across these regions.

As an alternative to the sink treatment, we consider an opposite end-member scenario in which meltwater remains dynamically connected across gaps within the ice-shelf domain (Fig. 1b). In these cells, LADDIE continues to solve for its prognostic variables: layer velocity, temperature, salinity, and thickness. Because melt rates are physically constrained by the local availability of glacial ice (sea ice is not explicitly represented in LADDIE), no melting occurs within the ice-shelf gaps. Consequently, no local meltwater volume or buoyancy is added to the flow in these areas. Nevertheless, the meltwater current advects temperature and salt across these gaps, allowing heat and momentum to be transported downstream. As a result, when the flow re-enters an ice-shelf-covered region, it can again drive sub-shelf melting and contribute to downstream melting.

In summary, the default configuration treats ice-shelf gaps as sinks of heat and momentum, whereas the alternative approach allows heat and momentum to be dynamically transported across open regions, directly affecting the downstream ice-shelf-covered regions. In the remainder of this paper, we will refer to the default configuration as the **sink** treatment and the alternative approach as the **connected** treatment.

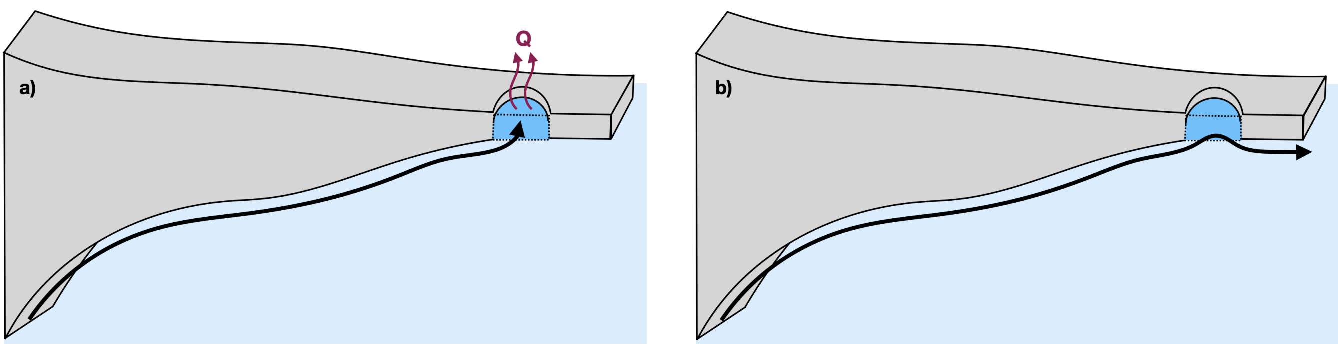

Figure 1. Schematic illustration of the two meltwater-flow treatments considered in this study. In the **sink** treatment (default LADDIE), meltwater flow loses its heat (Q) and momentum (black arrow) upon entering an ice-free region and therefore does not contribute to downstream meltwater transport (a). In the newly introduced **connected** treatment, meltwater flow remains dynamically connected across ice-free regions within the original ice-shelf mask, allowing heat and momentum to be transported downstream (b).

https://doi.org/10.5194/egusphere-2026-4237
Preprint. Discussion started: 2 September 2026
© Author(s) 2026. CC BY 4.0 License.

2.1.2 Ice-sheet model UFEMISM

To analyse the ice-dynamical sensitivity to the different representations of meltwater flow across ice-shelf gaps in LADDIE, we use a coupled setup with the ice-sheet model UFEMISM version 2.0 (Berends et al., 2025). The two models are fully integrated within a single code base (UPSY) and are discretised on the same unstructured mesh. In this study, UFEMISM is configured using the depth-integrated viscosity approximation (DIVA) to compute ice dynamics over both grounded and floating ice (Goldberg, 2011). Ice flow is represented using a single sliding law, namely the Coulomb-limited modified power-law formulation of Schoof (2005).

In UFEMISM, neither damage nor fracturing is included, and no explicit calving laws are applied. As a result, ice-shelf gaps only emerge when ice advection is insufficient to balance sub-shelf and surface melting. In the presented experiments, a constant positive surface mass balance is prescribed; consequently, sub-shelf melting is the sole mechanism responsible for the formation of open areas within the ice shelf. A minimum ice thickness of 1 m is imposed in UFEMISM. Grid cells with ice thickness below this threshold are removed to prevent numerical instabilities in the ice-dynamical solver.

2.2 Experiment design

2.2.1 Model geometry and initialisation

Our experiments are conducted in an idealised configuration based on the MISMIP+ experimental protocol (Asay-Davis et al., 2016). The geometry represents a symmetric ice stream feeding into a confined ice shelf. The bathymetry is described in detail in Asay-Davis et al. (2016). The simulations are performed at horizontal resolutions of 2 km and 1 km, where the stated resolution corresponds to the maximum triangle edge length. They are initialised from a 100 m thick ice slab, which thickens over time under a spatially uniform and constant surface mass balance of 0.3 m yr^{-1}. No sub-shelf melting is applied during the spin-up phase. A fixed calving front is prescribed at X = 640 km, and ice flowing across the calving front is immediately removed. The model is spun up for 40,000 years to reach a stable grounding-line position at approximately X = 450 km (see Asay-Davis et al. (2016) for geometric details) by tuning the ice rheology flow factor (A). This yields calibrated flow factors of $A = 1.94 \times 10^{-17}$ for the 2 km experiments and $A = 2.02 \times 10^{-17}$ for the 1 km experiments. After the spin-up, the flow factor is held fixed for all subsequent experiments.

2.2.2 LADDIE initialisation and tuning

We follow the tuning protocol of Asay-Davis et al. (2016) to initialise and calibrate LADDIE. The model is forced with the spun-up ice geometry and an idealised warm linear temperature and salinity profile (ISOMIP+ warm from Asay-Davis et al. (2016)), and the heat transfer coefficient (Γ_T) is adjusted such that the domain-averaged deep melt rate matches the ISOMIP+ target of 30 $\pm$ 1 m yr^{-1} in the high-melt scenario. Here, the deep region is defined as the area where the ice-shelf draft is below -300 m, consistent with the ISOMIP+ definition. A value of $\Gamma_T = 3.0 \times 10^{-2}$ was found to provide good agreement across both the 1 km and 2 km resolution experiments. Following the protocol, the salt transfer coefficient is prescribed as

https://doi.org/10.5194/egusphere-2026-4237
Preprint. Discussion started: 2 September 2026
© Author(s) 2026. CC BY 4.0 License.

$\Gamma_S = \Gamma_T/35$. The turbulent heat and salt exchange velocities are then computed as $\gamma_T = \Gamma_T U^*$ and $\gamma_S = \Gamma_S U^*$, respectively, where U^* denotes the friction velocity. An overview of all LADDIE model parameters and settings is provided in Table A1.

2.2.3 Coupled settings

Both LADDIE and UFEMISM are discretised on the same mesh and therefore have the same horizontal resolution. The models are coupled through the exchange of ice geometry (output from UFEMISM, input to LADDIE) and sub-shelf melt rates (output from LADDIE, input to UFEMISM), following the framework described by Lambert et al. (2026) (their Fig. 2).

In our experiments, coupling occurs at each UFEMISM time step (0.125 yr), corresponding to a coupling frequency of eight times per model year. LADDIE is integrated with a time step of 100 s. For the spun-up geometry obtained from the procedure described in Sect. 2.2.1, LADDIE is first run for 20 model days to reach a quasi-equilibrium state under the prescribed ocean forcing. Thereafter, LADDIE is run for 4 model days at each coupling step. This run duration is sufficient for the cavity size and forcing conditions considered in this study, as the flushing timescale of the meltwater layer is short relative to the coupling interval and changes in ice geometry over the 0.125 yr coupling interval remain limited (Jesse et al., 2025).

2.2.4 Experiments

The spun-up ice geometry and the calibrated tuning parameters (namely the ice rheology flow factor, A, in UFEMISM and the heat transfer coefficient, Γ_T, in LADDIE) serve as the initial conditions and reference model configuration for all experiments.

We perform simulations under three idealised ocean states, each characterised by a cold, fresher surface layer and a warmer, more saline deep layer, separated by a thermocline centred at 450 m depth. In all cases, the temperature profile follows a hyperbolic tangent function, while salinity is prescribed such that the resulting density profile is identical across the three ocean states. The experiments are denoted *ocean1*, *ocean2*, and *ocean3*, corresponding to deep-ocean temperatures of $-1.0°\mathrm{C}$, $0.0°\mathrm{C}$, and $1.0°\mathrm{C}$, respectively. For all experiments, the surface temperature is fixed at $-1.8°\mathrm{C}$ and the surface salinity at 34.0 psu. The vertically varying profiles are uniform in horizontal space and remain constant over time. The resulting forcing profiles are shown in Fig. S1.

To investigate the sensitivity to the treatment of open areas within the ice-shelf domain, we consider two model configurations: the **sink** treatment (Fig. 1a) and the **connected** treatment (Fig. 1b), as described in detail in Sect. 2.1.1. To assess the sensitivity of the results to model resolution, all experiments are conducted at two horizontal resolutions (1 km and 2 km). Combining the three ocean states, two meltwater flow treatments, and two model resolutions yields a total of 12 simulations.

3 Results

3.1 Connected meltwater flow across gaps enhances ice-sheet volume loss

Ice-volume sensitivity to the two different treatments of meltwater flow across ice-shelf gaps increases under warmer ocean conditions and at higher model resolution (Fig. 2). This increase reflects more frequent melt-through events under warm

https://doi.org/10.5194/egusphere-2026-4237
Preprint. Discussion started: 2 September 2026
© Author(s) 2026. CC BY 4.0 License.

forcing, due to enhanced melt rates, and at higher resolution, where sharper and more localised peak melt rates promote stronger spatially focused melting. In contrast, melt-through is rare in colder ocean scenarios, such that the meltwater flow treatment across gaps has little impact on simulated ice-volume loss in those cases.

In simulations where the two treatments diverge strongly (red lines in Fig. 2a, red and orange lines in Fig. 2b), allowing the meltwater flow to continue across ice-shelf gaps (connected) leads to enhanced ice-volume loss compared to when the meltwater flow loses its heat and momentum when encountering a gap (sink). This effect is substantially larger at 1 km resolution, where allowing meltwater flow to remain connected increases ice-volume loss by 2274 Gt (+38.63%) after 200 years relative to the sink treatment in the *ocean3* experiment. At 2 km resolution, the corresponding increase is only 729 Gt (+9.87%).

The much larger sensitivity at 1 km than at 2 km resolution reflects the lower frequency of melt-through events at 2 km resolution. The coarser resolution appears insufficient to resolve the coupled effects of focused melt patterns and limited ice advection that lead to gap formation, thereby reducing the sensitivity of ice-volume loss to the treatment of meltwater flow across these gaps. A sensitivity test at higher (750 m) resolution produces melt-through events at a frequency similar to that of the 1 km simulation and yields a comparable increase in ice-volume loss between the connected and sink treatments (2055 Gt, +34.91%). This convergence of the 750 m and 1 km results suggests that the 1 km resolution is sufficient to capture the relevant gap-forming processes and indicates that the enhanced ice loss is a robust feature of the meltwater-flow treatment rather than a numerical artifact of the 1 km resolution.

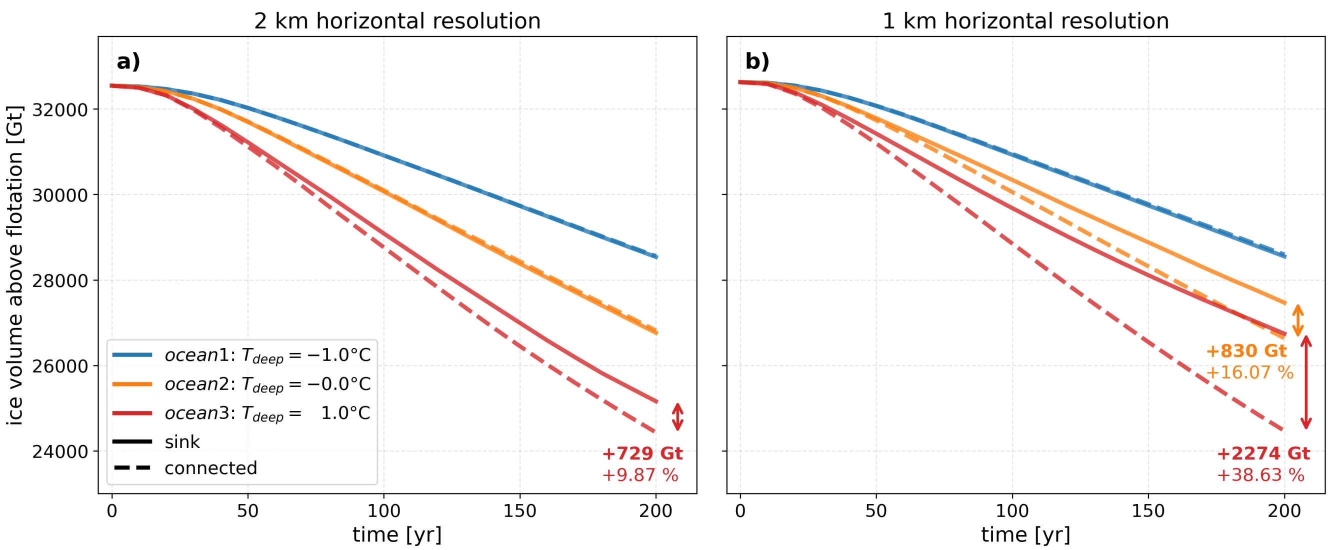

Figure 2. Ice volume above flotation for simulations with horizontal resolutions of 2 km (a) and 1 km (b). Colours indicate different ocean forcings, and solid and dashed lines distinguish the two meltwater treatments. Bold numbers show the additional ice-volume loss in the connected case relative to the sink case, calculated as the difference in total ice-volume loss after 200 years; the percentage increase relative to the sink treatment is also given.

https://doi.org/10.5194/egusphere-2026-4237
Preprint. Discussion started: 2 September 2026
© Author(s) 2026. CC BY 4.0 License.

Interestingly, after 200 years, cases with sustained downstream meltwater transport under moderate forcing and cases with interrupted transport under warmer forcing converge to similar ice volumes above flotation (dashed orange and solid red in Fig. 2b). This suggests that the impact of how meltwater flow is transmitted across ice-shelf gaps is comparable in magnitude to a 1°C difference in ocean temperature forcing at this 200-year timescale and 1 km model resolution.

Lastly, ice-volume loss is more consistent between the two model resolutions when meltwater flow remains connected across open ice-shelf areas (dashed lines in Fig. 2a,b), compared to when it is interrupted (solid lines in Fig. 2a,b). This suggests that sustained transport of heat and momentum across ice-shelf gaps reduces sensitivity to model resolution, whereas disruption of this transport enhances it.

3.2 Feedbacks arising from meltwater transport across gaps

To understand why allowing meltwater flow to continue across ice-shelf gaps enhances ice-volume loss relative to letting heat and momentum escape upon encountering gaps, we analyse the *ocean3* simulations at 1 km resolution in more detail (Fig. 3). The same qualitative behaviour is also found in the *ocean3* simulations at 2 km resolution (Fig. S2) and in the *ocean2* simulations at 1 km resolution (Fig. S3).

Initially, before gaps develop in the ice shelf, both simulations show the same melt pattern (Fig. 3i,m). The spatial variability is largely driven by the meltwater layer velocities, which show a strong boundary current along the western shear margin (Fig. 3q,u) due to Coriolis deflection of the meltwater flow. This results in elevated melt rates beneath the western shear margin.

By year 50, these elevated melt rates have become sufficient to generate gaps along the western shear margin of the ice shelf (Fig. 3b,f). The distinct treatment of meltwater flow around regions with ice-shelf gaps is clearly visible in the layer velocity fields (Fig. 3r,v). Allowing loss of heat and momentum from the system upon encountering gaps (sink) causes high layer velocities to terminate abruptly at the gaps, disrupting persistent downstream flow along the western margin (Fig. 3r). This interruption of the meltwater flow also reduces thermal driving farther downstream (Fig. S4), limiting the oceanic heat available for further melting. Together, the reduced layer velocities and thermal driving limit intense sub-shelf melting along the downstream western margin (Fig. 3j), ultimately restricting the region of thin ice to a small area near the deep western grounding line (Fig. 3b). The thicker downstream ice provides buttressing through its strong connection to the grounded western margin, thereby limiting ice velocities across the wider ice shelf (Fig. 3z).

In contrast, allowing continued meltwater flow across the gaps (connected) sustains strong meltwater flow (Fig. 3v) and maintains elevated thermal driving downstream of the gap (Fig. S4). Together, the sustained layer velocities and enhanced thermal driving promote intense sub-shelf melting along the downstream western margin (Fig. 3n), yielding a thinner, and locally open, western margin (Fig. 3f). The lack of thick ice limits buttressing from the grounded western margin, allowing persistently high ice velocities across the shelf (Fig. 3ad).

After 100 years, continued meltwater flow across the gaps results in persistent flow along the western margin (Fig. 3w), driving high sub-shelf melt rates beneath it (Fig. 3o). These high melt rates sustain the gap within the western shear margin (Fig. 3g) and support elevated ice velocities (Fig. 3ae). In contrast, loss of heat and momentum upon encountering gaps leads to low layer velocities along the western margin (Fig. 3s), coinciding with reduced melt rates (Fig. 3k). This lack of melting allows

https://doi.org/10.5194/egusphere-2026-4237
Preprint. Discussion started: 2 September 2026
© Author(s) 2026. CC BY 4.0 License.

localised thinning near the deep western grounding line to persist, while the downstream western margin thickens relative to its 50-year state (Fig. 3c). After 200 years, these spatial differences become even more pronounced: the western margin remains

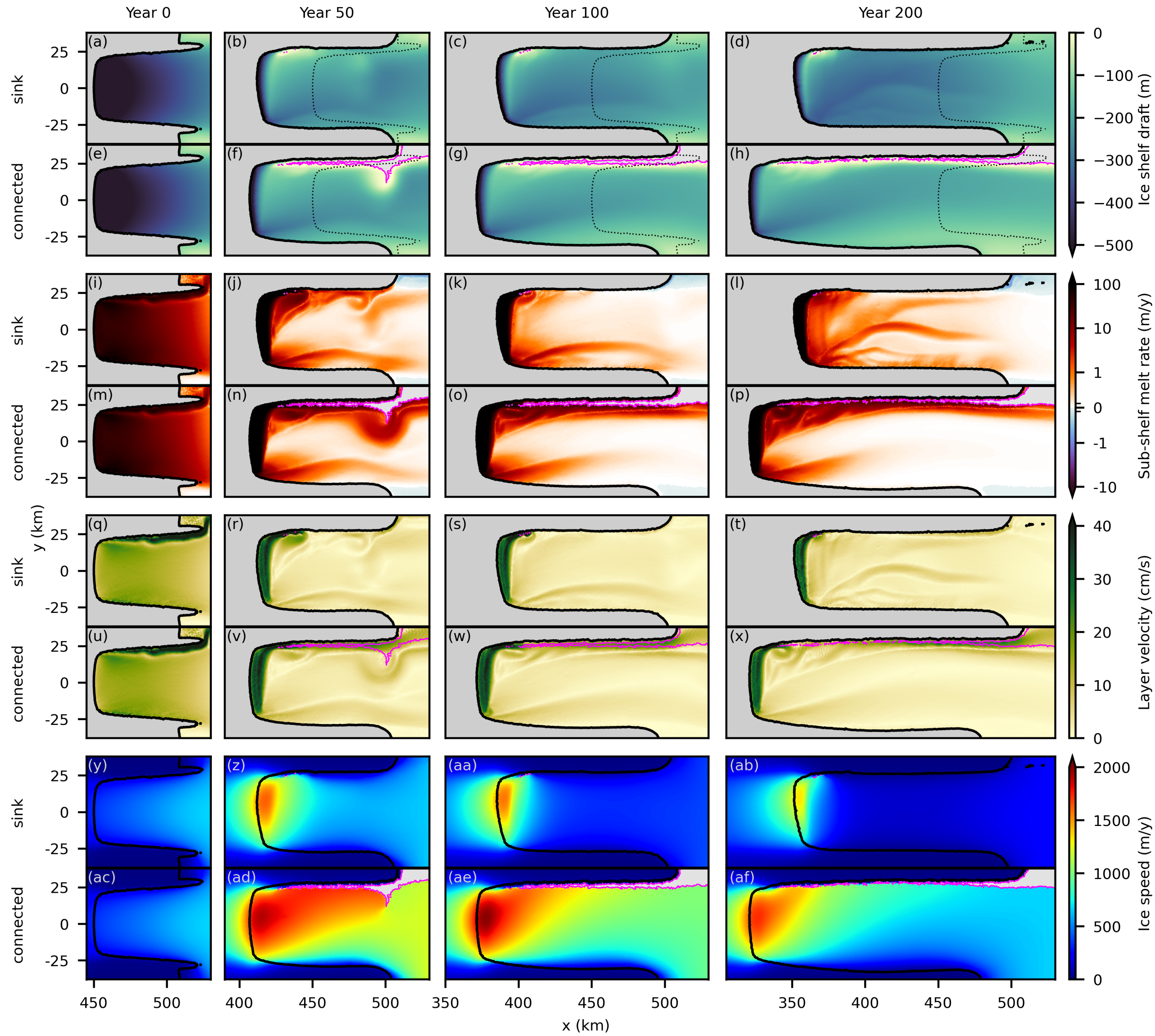

Figure 3. Spatial fields from the 1 km resolution *ocean3* simulations at selected time slices (columns). Shown are ice-shelf draft (rows 1–2), sub-shelf melt rates (rows 3–4), meltwater-layer velocity magnitude (rows 5–6), and ice speed (rows 7–8). For each variable, the upper row shows the 'sink' treatment, while the lower row shows the 'connected' treatment. Solid black lines represent the grounding line position, the dotted black lines (b-d and f-h) show the initial grounding line position (a and e). Solid magenta lines represent the ice shelf edge.

https://doi.org/10.5194/egusphere-2026-4237
Preprint. Discussion started: 2 September 2026
© Author(s) 2026. CC BY 4.0 License.

largely open where meltwater flow is sustained across open areas, whereas it continues to thicken where this flow is disrupted, leading to a stark contrast in ice velocities between the two meltwater-flow representations (Fig. 3ab,af).

In summary, these simulations reveal two contrasting feedback mechanisms. When ice-shelf gaps are treated as a sink to the meltwater flow, a negative feedback emerges: the occurrence of ice-shelf gaps suppresses downstream melt-through because the removal of heat and momentum disrupts the meltwater flow. This disruption can even promote ice thickening downstream of the gaps. Where regions downstream of gaps are important for ice-shelf stability, this feedback limits ice-flow acceleration, consistent with the behaviour described by Jesse et al. (2025). In contrast, when meltwater flow is allowed to continue across ice-free regions, a positive feedback develops: the sustained downstream transport of heat and momentum supports high melt rates farther along the margin, promoting additional thinning and more extensive melt-through. Where the affected regions contribute significantly to ice-shelf stability, this feedback reduces buttressing, accelerates ice flow, and enhances mass loss.

4 Discussion

4.1 Controls of ocean forcing, mesh resolution, and ice-shelf geometry

We find that the sensitivity to the treatment of meltwater flow across ice-shelf gaps increases when the model resolution is sufficiently high to resolve melt-through events, and further increases under warmer ocean conditions, which promote more frequent melt-through events. This indicates that model resolution and ocean forcing jointly control when and where the representation of meltwater flow becomes important. Notably, at 1 km resolution, the resulting sensitivity is comparable in magnitude to that induced by a 1°C change in ocean forcing, highlighting that the choice of meltwater representation can constitute a first-order source of uncertainty in studies using similar coupled ice-sheet–meltwater-layer models.

The impact of meltwater connectivity may also depend strongly on the specific ice-shelf geometry. In our experiments, allowing meltwater flow to continue across ice-shelf gaps increased melt rates beneath sectors of the ice shelf that provide substantial buttressing to the grounded ice sheet, thereby amplifying ice loss. For alternative geometries, however, gaps might develop away from regions of high buttressing importance, reducing the dynamical consequences of continued meltwater transport. The magnitude of the response is therefore not universal; instead, the resulting dynamical consequences are determined by whether these ice-shelf gaps happen to align with regions that are important for buttressing.

4.2 Mechanisms of ice-shelf gap formation

In our simulations, local gaps within the ice shelf arise solely through melt-through caused by intense sub-shelf melting. In reality, however, such gaps could form much earlier via damage and fracture processes (Lhermitte et al., 2020). Because these mechanical processes are not represented in our current model configuration, our setup likely provides a conservative estimate of when ice-shelf gaps start to occur. If fracture and calving processes were included, gaps might develop earlier during initial ice-shelf weakening, causing meltwater connectivity to become relevant sooner in the ice-sheet response. However, damage-induced weakening of shear margins could also reduce buttressing (Blasco et al., 2026), leading to greater ice-flow acceleration, particularly in the sink case, where the ice shelf remains attached, whereas in the connected case detachment has already reduced buttressing. This additional acceleration could potentially offset some of the enhanced ice loss caused by meltwater connectivity.

It is important to note that breakup through fracturing or calving does not result in clean, smooth pools of open ocean water. Instead, these processes leave behind rough, fragmented areas filled with sea ice, ice mélange, or trapped icebergs (Larour et al., 2021). Such areas inevitably disturb the meltwater flow, inducing heavy friction and partially dissipating heat and momentum. Consequently, neither our sink nor our connected approach is likely to be fully realistic there. Rather than representing the truth, these two configurations should be viewed as end-members that bracket the plausible range of sub-shelf meltwater connectivity. Crucially, this transport likely depends on the opening mechanism itself: while melt-through typically implies that the surrounding ice is also thin and transitioning gradually, mechanical damage can carve sharp rifts into thick ice, creating much steeper local thickness gradients that alter the meltwater circulation differently.

Targeted observations and high-resolution 3D ocean modelling will be critical to constrain exactly how much heat and momentum can be transported across these partially disrupted ice-shelf cavities. Such research would provide the physical basis for developing a more realistic representation of meltwater flow beneath ice shelves containing gaps in LADDIE, ultimately improving future ice-mass loss projections when coupled back to an ice dynamical model.

4.3 Different regimes of ice-shelf gaps: isolated vs. connected to the open ocean

One modelling choice we made is the way our connected treatment handles ice-free cells that connect to the open ocean. For those cells, we still allow the meltwater flow to continue. However, one could also argue that once there is a direct connection to the open ocean, the meltwater would be able to lose its heat and momentum more efficiently than in an internal ice-shelf gap that is more isolated. By maintaining connectivity across these open areas anyway, our setup deliberately tests the extreme upper bound of meltwater transport. This allows us to isolate the maximum potential feedback on downstream sub-shelf melting before more complex, intermediate boundary conditions are introduced.

For the experiments considered here, however, the local geography heavily limits any unphysical artifacts from this extreme treatment. The areas that ultimately connect to the open ocean are either located beyond X = 500 km, where the ice shelf is no longer laterally confined and changes have negligible implications for buttressing, or they develop within sheltered sectors between the ice shelf and the western grounded margin. In the latter case, the isolated nature of the embayment could facilitate the formation of fast ice, which restricts local exchange with the atmosphere, supporting meltwater connectivity as a physically reasonable approximation for these zones.

4.4 Parallels to observed ice-shelf geometries

While the geometry of our idealised experiments does not directly correspond to realistic ice-shelf configurations, similar geometric features can be identified in real systems. For instance, at Crosson Ice Shelf, observations of polynyas at the calving front of the Coriolis-favoured shear margin indicate active sub-shelf meltwater outflow beneath this sector (Alley et al., 2019). This margin also exhibits regions of extensive ice-shelf opening, observed as being filled with sea ice in satellite imagery, and is

https://doi.org/10.5194/egusphere-2026-4237
Preprint. Discussion started: 2 September 2026
© Author(s) 2026. CC BY 4.0 License.

characterized by high ice velocities (Lilien et al., 2018). This closely resembles our warm-ocean scenario configuration where meltwater transport persists dynamically across ice-free regions (Fig. 3; connected case), suggesting that continued meltwater connectivity may best capture the dynamics at Crosson Ice Shelf.

In contrast, Pine Island Ice Shelf more closely resembles the geometry of the sink configuration, in which heat and momentum can exit the cavity (Fig. 3; sink case). Extensive areas of thin ice and structural damage, including transient gaps, have been observed close to the deep grounding line within its southern shear zone (Lhermitte et al., 2020; Lowery et al., 2026). This highly localised, thin region closely mirrors the spatial geometry observed near the deep western grounding line in Fig. 3b-d, where localised thinning is immediately followed downstream by a thicker ice section. However, a polynya is frequently observed near the southern ice-shelf margin (Lhermitte et al., 2020), suggesting that some meltwater transport persists towards the ice-shelf front. Thus, while the geometry of Pine Island closely resembles the sink configuration, its meltwater transport may retain some degree of connectivity. Because the southern shear zone of Pine Island exerts a strong buttressing control on the grounded ice sheet (Naughten et al., 2023), the response of meltwater flow to the observed gaps could strongly influence large-scale ice dynamics.

The resemblance of Crosson to our connected treatment, and the closer similarity of Pine Island to the sink treatment while retaining some degree of meltwater connectivity, suggests that while both simplified meltwater treatments are unlikely to represent real systems exactly, different ice shelves may lean closer to one end-member or the other. This comparison suggests that realistic systems likely span a spectrum between these two regimes, governed by the interplay of local geometry and regional ocean forcing.

5 Conclusions

In coupled ice–sheet–meltwater-layer simulations within an idealised geometry, the treatment of local ice-shelf gaps in the computation of meltwater flow substantially affects the simulated ice-dynamical response, resulting in different magnitudes of ice-volume loss under identical ocean forcing conditions. When treating ice-shelf gaps as a sink for the meltwater current, downstream melting is suppressed, leading to reduced ice-volume loss relative to a configuration where meltwater transport is allowed to continue across these open areas. This sensitivity increases with the occurrence of these gaps, becoming more pronounced under warmer ocean conditions and when the model resolution is sufficient to resolve the coupled melt patterns and ice dynamics that produce these gaps.

Because our configurations deliberately represent two end-member cases by testing a localised sink and an extreme upper bound of sustained connectivity, the physically most realistic representation likely lies between these two idealised treatments. The ice dynamical sensitivity highlights that constraining how heat and momentum are transported across (distinct types of) partially disrupted cavities should remain a key target for future observations and high-resolution 3D ocean modelling.

Until these processes are fully understood and incorporated in models, our findings suggest that future modelling studies using meltwater layer models coupled to ice-sheet models should explicitly assess the sensitivity of their results to the treatment

https://doi.org/10.5194/egusphere-2026-4237
Preprint. Discussion started: 2 September 2026
© Author(s) 2026. CC BY 4.0 License.

of these regions. This is particularly critical for simulations investigating warm ocean states or employing high-resolution
285 configurations, where the frequent occurrence of ice-shelf gaps significantly amplifies the choice of meltwater representation.

Code and data availability. The code for the model versions used in this study, as well as configuration files and the model output is available via Zenodo: https://doi.org/10.5281/zenodo.21295945.

https://doi.org/10.5194/egusphere-2026-4237
Preprint. Discussion started: 2 September 2026
© Author(s) 2026. CC BY 4.0 License.

Appendix A: LADDIE model parameters

Table A1. LADDIE model parameters. PMP = pressure melting point.

parameter	description	default value	unit
f	Coriolis frequency	-1.37×10^{-4}	s^{-1}
g	gravitational acceleration	9.81	m s^{-2}
ρ_0	reference seawater density	1027	kg m^{-3}
ρ_{ice}	reference ice density	917	kg m^{-3}
$C_{d,mom}$	momentum drag coefficient	2.5×10^{-3}	-
$C_{d,top}$	top drag coefficient	2.5×10^{-3}	-
Γ_T	heat transfer coefficient	3.0×10^{-2}	-
Γ_S	salt transfer coefficient	$\Gamma_T/35$	-
α	thermal expansion coefficient	3.733×10^{-5}	°C^{-1}
β	haline contraction coefficient	7.843×10^{-4}	psu^{-1}
C_p	heat capacity of seawater	3974	J kg^{-1} °C^{-1}
L	latent heat of fusion	3.34×10^{5}	J kg^{-1}
C_I	heat capacity of ice	2009	J kg^{-1} °C^{-1}
λ_1	PMP salinity parameter	-5.73×10^{-2}	°C psu^{-1}
λ_2	PMP offset parameter	8.32×10^{-2}	°C
λ_3	PMP depth parameter	7.61×10^{-4}	°C m^{-1}
ν_0	kinematic viscosity	1.95×10^{-6}	m^2s^{-1}
A_h	viscosity parameter	10	m^2s^{-1}
K_h	diffusivity parameter	10	m^2s^{-1}
Pr	molecular Prandtl number	13.8	-
Sc	molecular Schmidt number	2432	-
μ	entrainment parameter	2.5	-
H_{min}	minimum layer thickness	1.0	m

https://doi.org/10.5194/egusphere-2026-4237
Preprint. Discussion started: 2 September 2026
© Author(s) 2026. CC BY 4.0 License.

Author contributions. FJ, EL, and RSvdW developed the study concept. EL and CJB developed the numerical models used in this study. FJ implemented the connected meltwater treatment, designed and conducted the experiments, performed the data analyses, produced the figures, and wrote the initial manuscript. All authors contributed to decisions regarding the model setup, discussed the results, and provided feedback on the manuscript.

Competing interests. The contact author has declared that none of the authors has any competing interests.

Acknowledgements. The authors thank Jan De Rydt for his valuable comments as editor on a previous manuscript, which motivated the further investigation of this process. Franka Jesse used AI tools such as Claude and ChatGPT to enhance the readability of specific paragraphs. Following this, the content was reviewed and edited as necessary. Full responsibility is taken for the final publication.

https://doi.org/10.5194/egusphere-2026-4237
Preprint. Discussion started: 2 September 2026
© Author(s) 2026. CC BY 4.0 License.

References

Alley, K. E., Scambos, T. A., Alley, R. B., and Holschuh, N.: Troughs developed in ice-stream shear margins precondition ice shelves for ocean-driven breakup, Science Advances, 5, eaax2215, https://doi.org/10.1126/sciadv.aax2215, 2019.

Asay-Davis, X. S., Cornford, S. L., Durand, G., Galton-Fenzi, B. K., Gladstone, R. M., Gudmundsson, G. H., Hattermann, T., Holland, D. M., Holland, D., Holland, P. R., Martin, D. F., Mathiot, P., Pattyn, F., and Seroussi, H.: Experimental design for three interrelated marine ice sheet and ocean model intercomparison projects: MISMIP v. 3 (MISMIP+), ISOMIP v. 2 (ISOMIP+) and MISOMIP v. 1 (MISOMIP1), Geosci. Model Dev., p. 27, 2016.

Berends, C. J., Azizi, V., Bernales, J. A., and van de Wal, R. S. W.: The Utrecht Finite Volume Ice-Sheet Model (UFEMISM) version 2.0 – Part 1: Description and idealised experiments, Geoscientific Model Development, 18, 3635–3659, https://doi.org/10.5194/gmd-18-3635-2025, 2025.

Blasco, J., Coulon, V., Izeboud, M., Gregov, T., Li, Y., and Pattyn, F.: Fracture-driven weakening amplifies projected ice loss from West Antarctica, Proceedings of the National Academy of Sciences, 123, e2601529 123, https://doi.org/10.1073/pnas.2601529123, 2026.

Fraser, A. D., Wongpan, P., Langhorne, P. J., Klekociuk, A. R., Kusahara, K., Lannuzel, D., Massom, R. A., Meiners, K. M., Swadling, K. M., Atwater, D. P., Brett, G. M., Corkill, M., Dalman, L. A., Fiddes, S., Granata, A., Guglielmo, L., Heil, P., Leonard, G. H., Mahoney, A. R., McMinn, A., van der Merwe, P., Weldrick, C. K., and Wienecke, B.: Antarctic Landfast Sea Ice: A Review of Its Physics, Biogeochemistry and Ecology, Reviews of Geophysics, 61, e2022RG000 770, https://doi.org/10.1029/2022RG000770, _eprint: https://agupubs.onlinelibrary.wiley.com/doi/pdf/10.1029/2022RG000770, 2023.

Goldberg, D. N.: A variationally derived, depth-integrated approximation to a higher-order glaciological flow model, Journal of Glaciology, 57, 157–170, https://doi.org/10.3189/002214311795306763, 2011.

Holland, D. M. and Jenkins, A.: Modeling Thermodynamic Ice–Ocean Interactions at the Base of an Ice Shelf, https://journals.ametsoc.org/view/journals/phoc/29/8/1520-0485_1999_029_1787_mtioia_2.0.co_2.xml, 1999.

Holland, P. and Feltham, D. L.: The Effects of Rotation and Ice Shelf Topography on Frazil-Laden Ice Shelf Water Plumes, Journal of Physical Oceanography, 36, 2312–2327, https://doi.org/10.1175/JPO2970.1, 2006.

Jenkins, A., Nicholls, K. W., and Corr, H. F. J.: Observation and Parameterization of Ablation at the Base of Ronne Ice Shelf, Antarctica, https://doi.org/10.1175/2010JPO4317.1, 2010.

Jesse, F., Lambert, E., and van de Wal, R. S. W.: Sub-shelf melt pattern and ice sheet mass loss governed by meltwater flow below ice shelves, The Cryosphere, 19, 3849–3872, https://doi.org/10.5194/tc-19-3849-2025, 2025.

Lambert, E., Jüling, A., van de Wal, R. S. W., and Holland, P. R.: Modelling Antarctic ice shelf basal melt patterns using the one-layer Antarctic model for dynamical downscaling of ice–ocean exchanges (LADDIE v1.0), The Cryosphere, 17, 3203–3228, https://doi.org/10.5194/tc-17-3203-2023, 2023.

Lambert, E., Jesse, F., and Berends, C. J.: The one-Layer Antarctic model for Dynamical Downscaling of Ice–ocean Exchanges (LADDIE) version 2.0, EGUsphere, pp. 1–31, https://doi.org/10.5194/egusphere-2026-930, 2026.

Larour, E., Rignot, E., Poinelli, M., and Scheuchl, B.: Physical processes controlling the rifting of Larsen C Ice Shelf, Antarctica, prior to the calving of iceberg A68, Proceedings of the National Academy of Sciences, 118, e2105080 118, https://doi.org/10.1073/pnas.2105080118, 2021.

Lewis, E. L. and Perkin, R. G.: Ice pumps and their rates, Journal of Geophysical Research: Oceans, 91, 11 756–11 762, https://doi.org/10.1029/JC091iC10p11756, _eprint: https://agupubs.onlinelibrary.wiley.com/doi/pdf/10.1029/JC091iC10p11756, 1986.

https://doi.org/10.5194/egusphere-2026-4237
Preprint. Discussion started: 2 September 2026
© Author(s) 2026. CC BY 4.0 License.

Lhermitte, S., Sun, S., Shuman, C., Wouters, B., Pattyn, F., Wuite, J., Berthier, E., and Nagler, T.: Damage accelerates ice shelf instability and mass loss in Amundsen Sea Embayment, Proceedings of the National Academy of Sciences, 117, 24 735–24 741, https://doi.org/10.1073/pnas.1912890117, 2020.

Lilien, D. A., Joughin, I., Smith, B., and Shean, D. E.: Changes in flow of Crosson and Dotson ice shelves, West Antarctica, in response to elevated melt, The Cryosphere, 12, 1415–1431, https://doi.org/10.5194/tc-12-1415-2018, 2018.

Lowery, K., Holland, P. R., Dutrieux, P., Hogg, A. E., and Gourmelen, N.: Drivers of Basal Melt Variability for Pine Island Glacier Ice Shelf: Ocean Forcing Versus Geometric Feedback, Geophysical Research Letters, 53, e2025GL121 404, https://doi.org/10.1029/2025GL121404, _eprint: https://agupubs.onlinelibrary.wiley.com/doi/pdf/10.1029/2025GL121404, 2026.

Naughten, K. A., Holland, P. R., and De Rydt, J.: Unavoidable future increase in West Antarctic ice-shelf melting over the twenty-first century, Nature Climate Change, 13, 1222–1228, https://doi.org/10.1038/s41558-023-01818-x, 2023.

Pritchard, H. D., Ligtenberg, S. R. M., Fricker, H. A., Vaughan, D. G., van den Broeke, M. R., and Padman, L.: Antarctic ice-sheet loss driven by basal melting of ice shelves, Nature, 484, 502–505, https://doi.org/10.1038/nature10968, 2012.

Schoof, C.: The effect of cavitation on glacier sliding, Proceedings of the Royal Society A: Mathematical, Physical and Engineering Sciences, 461, 609–627, https://doi.org/10.1098/rspa.2004.1350, 2005.

Watkins, R. H., Bassis, J. N., Thouless, M. D., and Luckman, A.: High Basal Melt Rates and High Strain Rates Lead to More Fractured Ice, Journal of Geophysical Research: Earth Surface, 129, e2023JF007 366, https://doi.org/10.1029/2023JF007366, _eprint: https://agupubs.onlinelibrary.wiley.com/doi/pdf/10.1029/2023JF007366, 2024.

Wearing, M. G., Stevens, L. A., Dutrieux, P., and Kingslake, J.: Ice-Shelf Basal Melt Channels Stabilized by Secondary Flow, Geophysical Research Letters, 48, e2021GL094 872, https://doi.org/10.1029/2021GL094872, _eprint: https://agupubs.onlinelibrary.wiley.com/doi/pdf/10.1029/2021GL094872, 2021.

Zinck, A.-S. P., Lhermitte, S., Wearing, M. G., and Wouters, B.: Channelized melt beneath Antarctic ice shelves previously underestimated, Nature Climate Change, pp. 1–4, https://doi.org/10.1038/s41558-025-02537-1, 2026.